Suppression of Hall-Term Effects by Gyroviscous Cancellation in Steady Collisionless Magnetic Reconnection

A. Ishizawa* and R. Horiuchi
National Institute for Fusion Science, Toki 509-5292, Japan
(Received 17 January 2005; published 22 July 2005)

The formation of an ion-dissipation region, in which motions of electrons and ions decouple and fast magnetic reconnection occurs, is demonstrated during a steady state of two-dimensional collisionless driven reconnection by means of full-particle simulations. The Hall-term effect is suppressed due to the gyroviscous cancellation at scales between the ion-skin depth and ion-meandering-orbit scale, and thus ions are tied to the magnetic field. The ion frozen-in constraint is strongly broken by nongyrotropic pressure tensor effects due to ion-meandering motion, and thus the ion-dissipation region is formed at scales below the ion-meandering-orbit scale. A similar process is observed in the formation of an electron-dissipation region. These two dissipation regions are clearly observed in an out-of-plane current density profile.

DOI: 10.1103/PhysRevLett.95.045003 PACS numbers: 52.35.Vd, 52.65.Rr, 94.30.Ej

Collisionless magnetic reconnection is a fundamental mechanism for the rapid release of magnetic energy in solar corona, high temperature tokamaks, magnetospheric substorms, and laboratory plasmas [1–7]. Recent computer simulation studies have revealed that the rate of reconnection by collisionless processes is very large compared to those obtained by using resistive magnetohydrodynamics (MHD) [8]. Rapid reconnection is demonstrated to occur when the motions of electrons and ions decouple in a narrow region around the reconnection point, in two-fluid simulations, in hybrid simulations, and in full-particle simulations [8–16]. This decoupling is explained in terms of two-fluid effects and particle orbit effects, which are not included in the MHD model, and which form an ion-dissipation region. In this region the ion frozen-in condition is broken and the ions are unmagnetized, while the electrons are tied to the field [8–16]. This difference between the ion flow and electron flow causes fast magnetic reconnection because it leads to the generation of fast electron flows in the ion-dissipation region. We call the region, in which the plasma's frozen-in condition is violated, the dissipation region, although the violation is caused by collisionless effects. The violation dominantly controls the formation of the dissipation region and of the current density profile.

When the electrons are tied to the magnetic field in the ion-dissipation region, we expect that the ion frozen-in constraint is broken at scales below the ion-skin depth, because

$$\boldsymbol{E} + \boldsymbol{v}_e \times \boldsymbol{B} = \boldsymbol{E} + \boldsymbol{v}_i \times \boldsymbol{B} - \frac{d_i}{n}\boldsymbol{J} \times \boldsymbol{B} = \boldsymbol{0}, \quad (1)$$

where $\boldsymbol{J} = n/d_i(\boldsymbol{v}_i - \boldsymbol{v}_e)$, $\boldsymbol{v}_i$, $\boldsymbol{v}_e$, n, and $d_i = c/\omega_{pi}$ are the electric current, ion flow velocity, electron flow velocity, plasma density, and ion-skin depth, respectively. On the other hand, full-particle simulations show that the ion frozen-in condition is violated only within the ion-meandering-orbit scale in steady collisionless reconnection [17–19]. Note that the meandering motion is a bouncing motion in a field reversal region.

In this Letter, we work out this discrepancy between the two spatial scales controlling the ion-dissipation region: the ion-skin depth d_i suggested by the electron frozen-in condition and the ion-meandering-orbit scale l_{mi} suggested by full-particle simulations. We show that the ion pressure tensor plays two crucial roles in the formation of the ion-dissipation region. One role is by the gyroviscous pressure [20,21], which suppresses the violation of the frozen-in condition due to the inertia effect, so that the ions are almost tied to the field within d_i. The other role is played by the nongyrotropic pressure, which causes strong violation of the frozen-in condition within l_{mi}.

We analyze a steady state of collisionless driven reconnection without any guide field in an open system with the mass ratio $m_i/m_e = 800$ by using the two-dimensional electromagnetic particle-in-cell simulation code developed in our previous work [9,10,17,18]. The simulation domain is a square open region in the xy plane. At the upstream boundary, the ions and electrons are tied to the magnetic field, and thus the plasma inflow is driven by $\boldsymbol{E} \times \boldsymbol{B}$ drift due to an external electric field applied in the z direction [17]. The applied field takes a uniform profile with a constant value E_0 when the system relaxes to a steady state [17,18]. At the downstream boundary, the plasma can freely flow in or out [18]. The initial condition is given by a one-dimensional Harris-type equilibrium as $B_x(y) = B_0 \tanh(y/y_h)$ and $P(y) = B_0^2/8\pi\,\mathrm{sech}^2(y/y_h)$. We set the time step to be $\omega_{ce0}\Delta t = 0.02$ and use a 512×512 point grid and 25.6×10^6 particles.

Figure 1 shows the perspective view of the out-of-plane current density profile in the reconnection plane after the system relaxes to a steady state. The profile has a sharp peak at the center where reconnection occurs, and this point is called the X point. The current density profile along the inflow direction consists of two parts. One is a sharp peak and the other is a low shoulder. Figure 2 illus-

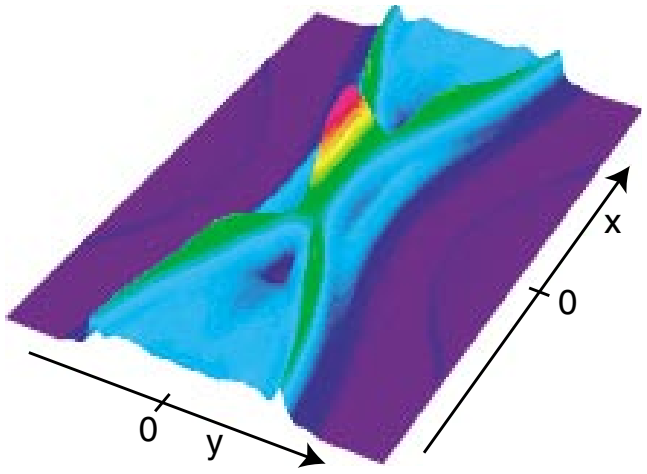

FIG. 1 (color). The perspective view of the out-of-plane current density profile on the xy plane in the steady state.

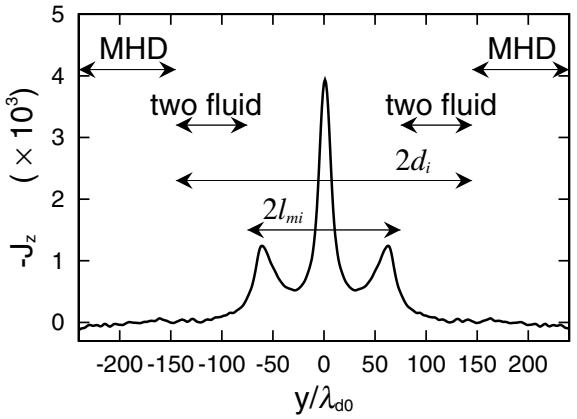

FIG. 2. The spatial profile of the out-of-plane current density along the vertical line passing the X point in the steady state.

trates this two-scale structure in detail, where λ_{d0} is the Debye length. The low shoulder is controlled by the ion-meandering-orbit scale l_{mi}, which satisfies $l_{mi} = \rho_i(l_{mi})$. This scale corresponds to the location where the local ion Larmor radius $\rho_i(y) \equiv v_{ti}(y)/\omega_{ci}(y)$ is equal to the scale length of the magnetic field $\rho_i(y) = L_B(y)$, where $L_B(y) = B_x/(\partial B_x/\partial y)$, and thus the ion dynamics is fully kinetic within l_{mi}. Note that the local ion cyclotron frequency $\omega_{ci}(y) \equiv \sqrt{eB(y)/m_i c}$ and the local ion thermal velocity $v_{ti}(y) \equiv \sqrt{T_i(y)/m_i}$ are evaluated by using the local magnetic field $B(y)$ and the local ion temperature $T_i(y)$ calculated from the particle velocities and particle positions. The sharp peak is formed through the electron dynamics. The current layer has no structure characterized by the ion-skin depth d_i, which is evaluated by using the averaged density in the current layer. Note that two-fluid effects should be included within this scale, while a MHD description is valid beyond this scale. We call the region between d_i and l_{mi} the two-fluid region.

We focus on the formation of the dissipation region that enables fast magnetic reconnection. Figure 3 shows the spatial profiles of various terms measuring the violation of the frozen-in condition along the vertical line passing through the X point in the steady state. The out-of-plane electric field E_z that is induced at the upstream boundary by the applied electric field $E_0 = -0.04B_0c$ spreads over the system and becomes uniform. The value of the electric field at the X point, $y = 0$, is the reconnection electric field. Figure 3(a) shows that $-\boldsymbol{v}_i \times \boldsymbol{B}$ is almost the same as the electric field at the outside of the region indicated by ion scales, and thus the ions are tied to the field. The ion frozen-in condition is strongly broken within the ion-meandering-orbit scale l_{mi}. On the other hand, the ions are almost tied to the field in the two-fluid region ($l_{mi} < y < d_i$), and correspondingly the Hall term $\boldsymbol{J} \times \boldsymbol{B}$ is small between d_i and l_{mi} and becomes large within l_{mi}. Figure 3(b) shows the relation $E_z = -\boldsymbol{v}_e \times \boldsymbol{B}|_z$ holds except near the Xpoint. This implies that the electrons are still tied to the field in the ion-dissipation region where the ion frozen-in condition is broken. This electron frozen-in condition implies the violation of the ion frozen-in condition within d_i as explained by making use of Eq. (1). We note that this electron frozen-in condition is consistent with the results of the Swarthmore spheromak experiment [7], which showed the electron inertia term is small in the region where the Hall term is large.

In order to investigate the violation mechanism of the frozen-in constraint in relation to the formation of the dissipation region, let us examine the nonideal terms in the momentum equations at steady state

$$\boldsymbol{E} + \boldsymbol{v}_i \times \boldsymbol{B} = \frac{d_i}{n}\nabla \cdot \boldsymbol{P}_i + d_i \boldsymbol{v}_i \cdot \nabla \boldsymbol{v}_i, \qquad (2)$$

$$\boldsymbol{E} + \boldsymbol{v}_e \times \boldsymbol{B} = -\frac{d_i}{n}\nabla \cdot \boldsymbol{P}_e - \frac{d_e^2}{d_i}\boldsymbol{v}_e \cdot \nabla \boldsymbol{v}_e, \qquad (3)$$

based on the particle simulation data, where $\boldsymbol{P}_i$ and $\boldsymbol{P}_e$ are the ion and electron pressure tensors, respectively. The normalizations are $\boldsymbol{v}/v_A \to \boldsymbol{v}$, $\boldsymbol{B}/B_0 \to \boldsymbol{B}$, $n/n_0 \to n$, $\boldsymbol{E}c/(v_A B_0) \to \boldsymbol{E}$, $\boldsymbol{x}/L \to \boldsymbol{x}$, $t/(L/v_A) \to t$, $\boldsymbol{P}/(B_0^2/4\pi) \to \boldsymbol{P}$, $\boldsymbol{J}/(cB_0/4\pi L) \to \boldsymbol{J}$, where $v_A = B_0/\sqrt{4\pi m_i n_0}$. Figures 3(c) and 3(d) show the spatial profiles of the out-of-plane component of the terms in Eqs. (2) and (3). It is worth noting that the ion pressure tensor term $\nabla \cdot \boldsymbol{P}_i$ cancels out the ion inertia term $\boldsymbol{v}_i \cdot \nabla \boldsymbol{v}_i$ in the two-fluid region ($l_{mi} < y < d_i$) where the ion inertia term is large and works toward breaking the frozen-in condition as shown in Fig. 3(c). Therefore, this cancellation leads to the suppression of the Hall-term effects and to the maintenance of the ion frozen-in constraint within d_i. The ion frozen-in condition is strongly broken, and the $\boldsymbol{v}_i \times \boldsymbol{B}$ term is small in the full kinetic region within l_{mi} where the pressure tensor term is dominant. This large pressure tensor term is originated from the nongyrotropic ion-meandering motion. The strong violation leads to the formation of the low shoulder of current density profile in

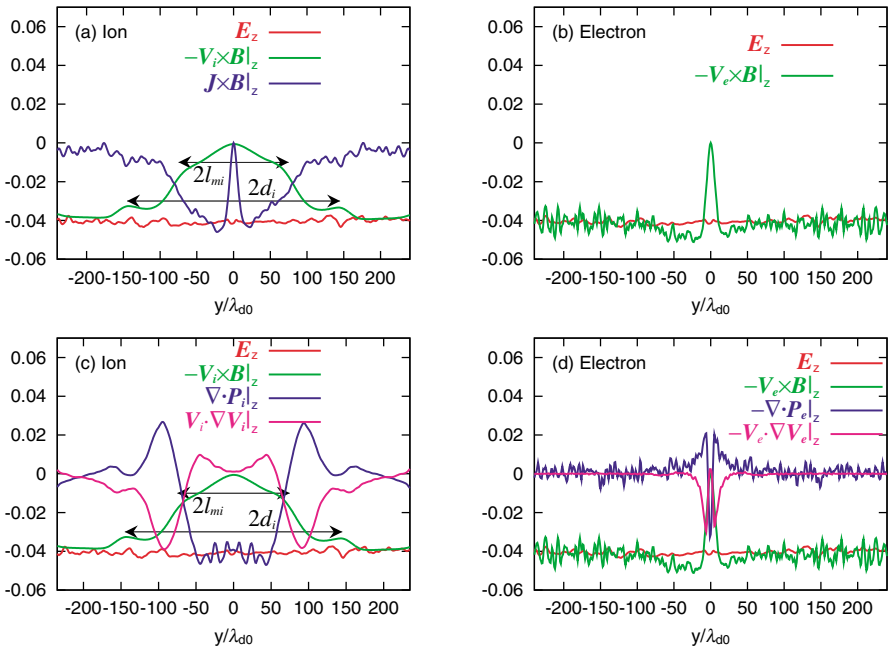

FIG. 3 (color). The spatial profile of each term in the out-of-plane component of the ion momentum equation and of the electron momentum equation along the vertical line passing the X point in the steady state.

Fig. 2. Note that the nongyrotropic part of the ion pressure tensor balances the electric field at the X point. Figure 3(d) shows that the electron pressure tensor term $\nabla\cdot\boldsymbol{P}_e$ and the electron inertia term $\boldsymbol{v}_e\cdot\nabla\boldsymbol{v}_e$ break the electron frozen-in constraint near the X point. The electron inertia term vanishes at the X point, while the electron pressure tensor term has a sharp peak, and it balances the electric field there. Thus, the reconnection electric field is generated by the nongyrotropic pressure tensor originating from the electron-meandering motion at the X point as suggested by Refs. [15,19]. The electron pressure tensor seems to cancel out the electron inertia effect in the region between d_e and l_{me}. Unfortunately, the cancellation is not clear because the electron-skin depth d_e is close to the electron-meandering-orbit scale l_{me} in our simulation. A similar counterbalance is also demonstrated in the simulation of electron-positron plasmas [22]. We summarize the violation of the frozen-in condition and the counterbalance in Table I.

TABLE I. Violation of frozen-in condition.

Violation of ion frozen-in condition		
$0<y<l_{mi}$	$l_{mi}<y<d_i$	$d_i<y$
$\boldsymbol{E}+\boldsymbol{v}_i\times\boldsymbol{B}=\nabla\cdot\boldsymbol{P}_i$	$\boldsymbol{E}+\boldsymbol{v}_i\times\boldsymbol{B}\cong\boldsymbol{0}$	$\boldsymbol{E}+\boldsymbol{v}_i\times\boldsymbol{B}=\boldsymbol{0}$
$\boldsymbol{v}_i\cdot\nabla\boldsymbol{v}_i\ll\nabla\cdot\boldsymbol{P}_i$	$\boldsymbol{J}\times\boldsymbol{B}\cong\nabla\cdot\boldsymbol{P}_i+\boldsymbol{v}_i\cdot\nabla\boldsymbol{v}_i\cong 0$	
	Gyroviscous cancellation	
Fully kinetic	Two-fluid region	MHD is valid
Violation of electron frozen-in condition		
$0\le y<l_{me}$	$l_{me}<y<d_e$	$d_e<y$
$\boldsymbol{E}+\boldsymbol{v}_e\times\boldsymbol{B}=-\nabla\cdot\boldsymbol{P}_e$	$\boldsymbol{E}+\boldsymbol{v}_e\times\boldsymbol{B}\cong\boldsymbol{0}$	$\boldsymbol{E}+\boldsymbol{v}_e\times\boldsymbol{B}=\boldsymbol{0}$
$\boldsymbol{v}_e\cdot\nabla\boldsymbol{v}_e\ll\nabla\cdot\boldsymbol{P}_e$	$\nabla\cdot\boldsymbol{P}_e+\boldsymbol{v}_e\cdot\nabla\boldsymbol{v}_e\cong 0$	

Let us consider how the ion pressure tensor compensates the frozen-in condition for the violation due to the ion inertia effect within the ion-skin depth. This effect is generated by the gyroviscous cancellation [20,21], which is a common property of magnetized plasmas and is caused by the finite-Larmor-radius effect,

$$n\frac{d\boldsymbol{v}_{di}}{dt}+(\nabla\cdot\boldsymbol{\pi}_{gv})_\perp=-\nabla_\perp\chi_g, \tag{4}$$

where $d/dt\equiv\partial/\partial t+\boldsymbol{v}_i\cdot\nabla$, $\boldsymbol{v}_i=\boldsymbol{v}_{\|i}+\boldsymbol{v}_{E\times B}+\boldsymbol{v}_{di}$, $(\nabla\cdot\boldsymbol{\pi}_{gv})_\perp\equiv(\nabla\cdot\boldsymbol{P})_\perp-\nabla_\perp p_\perp$, and subscripts $\|$ and $\perp$ denote parallel and perpendicular components. In this equation $\boldsymbol{v}_{E\times B}\equiv\boldsymbol{E}\times\boldsymbol{B}/B^2$, $\boldsymbol{v}_{di}\equiv\frac{d_i}{nB^2}\boldsymbol{B}\times\nabla p_i$, $\boldsymbol{\pi}_{gv}$, $p_\perp$, and χ_g are the $\boldsymbol{E}\times\boldsymbol{B}$ flow velocity, ion diamagnetic flow velocity, gyroviscous tensor, perpendicular pressure, and a correction of scalar pressure [21]. The out-of-plane component (the z component) of Eq. (4) at steady state is $\boldsymbol{v}_i\cdot\nabla\boldsymbol{v}_{diz}+\frac{1}{n}\nabla\cdot\boldsymbol{P}|_z=0$, where $\boldsymbol{A}|_z$ stands for a z component of $\boldsymbol{A}$ and the relations $\nabla_\perp\chi_g|_z=\nabla_\perp p_\perp|_z=0$ have been used because $\partial/\partial z=0$ in the two-dimensional system. Thus, Eq. (4) implies that the z component of the ion inertia term balances the pressure tensor term $\boldsymbol{v}_i\cdot\nabla\boldsymbol{v}_{iz}\cong\boldsymbol{v}_i\cdot\nabla\boldsymbol{v}_{diz}=-\frac{1}{n}\nabla\cdot\boldsymbol{P}|_z$ between d_i and l_{mi} because the ion flow velocity $\boldsymbol{v}_{iz}$ is dominated by the diamagnetic flow velocity $\boldsymbol{v}_{diz}$ for $l_{mi}<y<d_i$ as shown in Fig. 4. Therefore, the violation due to the ion inertia term is being counteracted by the gyrotropic pressure tensor term, and the Hall term is small,

$$\frac{1}{n}\boldsymbol{J}\times\boldsymbol{B}=\boldsymbol{v}_i\cdot\nabla\boldsymbol{v}_i+\frac{1}{n}\nabla\cdot\boldsymbol{P}_i+O(m_e/m_i)\cong O(m_e/m_i), \tag{5}$$

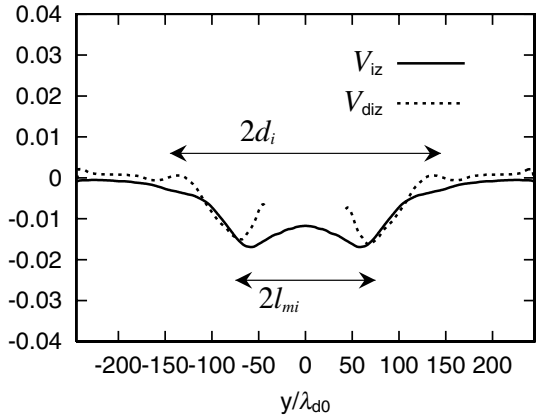

FIG. 4. The spatial profile of the out-of-plane ion flow velocity (solid line) and the out-of-plane ion diamagnetic flow velocity (dotted line) along the vertical line passing the X point in the steady state.

for $l_{mi} < y < d_i$. This cancellation should occur inside of d_i because it is the finite-Larmor-radius effect. Moreover, the cancellation should occur outside of l_{mi} because ions do not exhibit the Larmor motion within l_{mi}. Thus the cancellation mechanism works well only in the two-fluid region ($l_{mi} < y < d_i$) when $l_{mi} < d_i$.

In summary, we have worked out the discrepancy between the two spatial scales that can control an ion-dissipation region, where fast reconnection occurs, in steady collisionless reconnection. One is the ion-skin depth d_i predicted from the fact that electrons are tied to the magnetic field in the ion-dissipation region because of Eq. (1). The other is the ion-meandering-orbit scale l_{mi}, which is revealed from full-particle simulations. We found that gyroviscous cancellation occurs at scales between d_i and l_{mi}, and correspondingly the ion pressure tensor compensates the ion frozen-in condition for the violation due to the ion inertia effect. Therefore, the Hall term is small at scales between d_i and l_{mi}. The nongyrotropic pressure tensor effect due to the ion-meandering motion strongly violates the ion frozen-in condition within l_{mi}, and it dominantly controls the width of the ion-dissipation region. Hence, there exists the current layer controlled by the ion-meandering-orbit scale and no spatial structure characterized by the ion-skin depth in the current density profile during the steady state of collisionless reconnection. This result is consistent with the observed current layer width of $0.4d_i \approx \rho_i$ in the magnetic reconnection experiment [5]. Note that the difference between d_i and l_{mi} is not an order but a factor in our simulation. The difference should be large in low-β plasmas. We also note that the ion-skin depth controls the current layer width when the reconnection is unsteady as shown in Refs. [12,13,19].

A similar counterbalance is observed in the violation of the electron-frozen-in condition. Our numerical results suggest that the electron pressure tensor term counteracts the violation due to the electron inertia within the electron-skin depth, and thus the width of the electron-dissipation region is mainly controlled by the electron-meandering-orbit scale. Unfortunately, the counterbalance is not clear compared to that of the ions because the electron-skin depth is close to the electron-meandering-orbit scale in our simulations. The electron-dissipation region corresponds to the sharp peak in the current density profile, and thus we have the two-scale structure of the current layer as shown in Fig. 2.

We found that the cancellation occurs when the plasma β is about one and expect that the cancellation is universal when plasma β is less than one because the gyroviscous cancellation is a common property of magnetized plasmas. This would be examined from simulations of magnetic reconnection in low-β plasmas in future work.

The authors thank Professor M. Okamoto at the National Institute for Fusion Science for his encouragement and thank Professor E. Hameiri at New York University for his careful reading of this manuscript.

*Electronic address: ishizawa@nifs.ac.jp

[1] D. Biskamp, *Magnetic Reconnection in Plasmas* (Cambridge University Press, Cambridge, 2000).
[2] J. F. Drake, Nature (London) **410**, 525 (2001).
[3] Y. Ono, M. Yamada, T. Akao, T. Tajima, and R. Matsumoto, Phys. Rev. Lett. **76**, 3328 (1996).
[4] S. C. Hsu, G. Fiksel, T. A. Carter, H. Ji, R. M. Kulsrud, and M. Yamada, Phys. Rev. Lett. **84**, 3859 (2000).
[5] M. Yamada, H. Ji, S. Hsu, T. Carter, R. Kulsrud, and F. Trintchouk, Phys. Plasmas **7**, 1781 (2000).
[6] J. F. Drake and Y. C. Lee, Phys. Fluids **20**, 1341 (1977).
[7] C. D. Cothran, M. Landreman, M. R. Brown, and W. H. Matthaeus, Geophys. Res. Lett. **32**, L03105 (2005).
[8] J. Birn *et al.*, J. Geophys. Res. **106**, 3715 (2001).
[9] R. Horiuchi and T. Sato, Phys. Plasmas **1**, 3587 (1994).
[10] R. Horiuchi and T. Sato, Phys. Plasmas **4**, 277 (1997).
[11] B. N. Rogers, R. E. Denton, J. F. Drake, and M. A. Shay, Phys. Rev. Lett. **87**, 195004 (2001).
[12] M. A. Shay, J. F. Drake, R. E. Denton, and D. Biskamp, J. Geophys. Res. **103**, 9165 (1998).
[13] M. A. Shay, J. F. Drake, B. N. Rogers, and R. E. Denton, J. Geophys. Res. **106**, 3759 (2001).
[14] M. A. Shay and J. F. Drake, Geophys. Res. Lett. **25**, 3759 (1998).
[15] M. Hesse, K. Schindler, J. Birn, and M. Kuznetsova, Phys. Plasmas **6**, 1781 (1999).
[16] M. M. Kuznetsova, M. Hesse, and D. Winske, J. Geophys. Res. **105**, 7601 (2000).
[17] W. Pei, R. Horiuchi, and T. Sato, Phys. Rev. Lett. **87**, 235003 (2001).
[18] W. Pei, R. Horiuchi, and T. Sato, Phys. Plasmas **8**, 3251 (2001).
[19] A. Ishizawa, R. Horiuchi, and H. Ohtani, Phys. Plasmas **11**, 3579 (2004).
[20] S. I. Braginskii, in *Reviews of Plasma Physics*, edited by M. A. Leontovich (Consultants Bureau, New York, 1965), Vol. I, p. 205.
[21] Z. Chang and J. D. Callen, Phys. Fluids B **4**, 1766 (1992).
[22] A. Bhattacharjee (private communication).